Analytical Methods

Accepted Manuscript

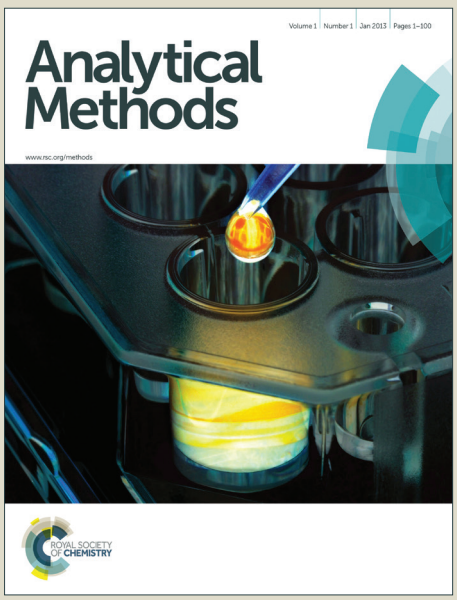

ROYAL SOCIETY OF CHEMISTRY

www.rsc.org/methods

A voltammetric sensor based on eosin Y film modified glassy carbon electrode for simultaneous determination of hydroquinone and catechol

Jiahong He[a,b,c], Ri Qiu[b], Wenpo Li[a], Shaohua Xing[b], Zhongrong Song[c], Qiang Li [c]*, Shengtao Zhang[a]*

a School of Chemistry and Chemical Engineering, Chongqing University, Chongqing 400044, P. R. China

b State key laboratory for marine corrosion and protection，Luoyang ship material research institute, Qingdao 266101, P. R. China

c School of Materials and Chemical Engineering, Chongqing University of Arts and Sciences, Yongchuan 402160, P. R. China

Contact information for Corresponding Author

Associate Professor Sheng-tao Zhang, School of Chemistry and Chemical Engineering, Chongqing University, Chongqing 400044, PR China

Fax: 86-23-65102531. Tel: +86-18602319242

E-mail: stzhang@cqu.edu.cn

* Corresponding author. Tel: +86-23-65102531.

Email: stzhang@cqu.edu.cn (Shengtao Zhang) ; 20110901036@ cqu.edu.cn (Qiang Li)

Abstract: By using cyclic voltammetry method, eosin Y film was electrodeposited on the surface of glassy carbon electrode (GCE) to obtain the modified electrode (denoted as eosin Y/GCE). Scanning electron microscopy, electrochemical impedance spectroscopy and cyclic voltammetry techniques were used for morphology and electrochemical property characterization of eosin Y/GCE. The electrocatalysis capability of eosin Y/GCE to hydroquinone (HQ) and catechol (CC) was investigated by cyclic voltammetry (CV) and differential pulse voltammetry (DPV) techniques. Compared with the bare GCE, eosin Y/GCE behaved an outstanding electrocatalytic activity and reversibility towards the oxidation of HQ and CC. The oxidation and reduction peak separation was decreased from 386 to 60 mV for HQ and from 340 to 56 mV for CC at eosin Y/GCE, respectively. The differential pulse voltammetry results showed that the oxidation peaks of the two isomers in acetate buffer solution could be clearly discriminated with a peak potential separation of *ca*. 106 mV, which was wide enough to discriminate the two dihydroxybenzene isomers. Under the optimal conditions, the oxidation peak currents were linear to HQ/ CC concentration in the range from 1 μM to 130 μM with the detection limit as 0.14 μM (3σ) for HQ and 0.12 μM (3σ) for CC, respectively. Moreover, eosin Y/GCE exhibited an excellent anti-interference ability. It was successfully applied to the simultaneous determination of HQ and CC in spiked water samples with reliable recovery.

Keywords: eosin Y; modified electrode; simultaneous determination; hydroquinone; catechol.

1. Introduction

Phenol compounds are important contaminants in nature, since they are the essential raw materials and byproducts of vast chemical industries. Hydroquinone (1,4-dihydroxybenzene, HQ) and catechol (1,2-dihydroxybenzene, CC) are two isomers of phenolic compounds, which are widely used in many fields such as cosmetics, antioxidant, tanning, pesticides, medicines and photography chemicals [1]. Even at very low concentration, the two isomers are highly toxic to human health and difficult to degrade in the ecological environment [2,3], so that they can be regarded as the hazard materials. In addition, since the two isomers often coexist and interference with each other due to their similar structure and physicochemical properties, direct simultaneous determination of the two isomers remains a challenge [4]. Thus, it is a thirst to develop simple, rapid and convenient analytical method to simultaneously determine both HQ and CC.

Until now, sophisticated analytical methods have been proposed for detecting and determining the two isomers, such as high performance liquid chromatography [5,6], synchronous fluorescence [7], spectrophotometry [8], chemiluminescence [9], capillary electrophoresis [10] and gas chromatography/mass spectrometry [11]. Although using these methods has been proven successfully for dihydroxybenzene determination, some drawbacks still exist, such as complex operating conditions, time-consuming processes, expensive equipments, and so forth. Compared with these traditional methods mentioned above, electrochemical methods are preferable and attractive for the simultaneous detection of such phenolic compounds due to the high accuracy, fast response, simple operation, low cost, high sensitivity, and excellent selectivity [12, 13]. If choosing conventional unmodified electrodes for detection, however, there are still a few shortcomings, e. g., high overpotential for oxidation of CC and HQ, poor detection selectivity, the overlapped oxidation/reduction peaks of the two isomers [14]. Thus, much effort has been devoted to utilizing versatile material as candidate to modify the electrode for improving the detection performance. These years, the new developed materials, such as graphene [15], carbon nanofiber [16], polyaniline/MnO_2 [17], multiwalled

carbon nanotubes-ionic liquid composite [18,19], carbon nanotube doped poly(3,4-ethylenedioxythhiophene) [20], graphene nanosheet-poly(4-vinyl pyridine) [21], poly(crystal violet)-graphene [22], polymeric ionic liquid- multiwalled carbon nanotubes [23], graphitic mesoporous carbon [24], ultrathin CdSe nanosheets [25], have been used as modified electrodes to explore their simultaneous voltammetric determination of HQ and CC. However, there are still some disadvantages accompanying with these electrocatalysts, e. g. high cost, complicated fabrication process, and poor reproducibility. Thus, it is still a challenge to achieve novel electrode material for the simultaneous determination of HQ and CC with high stability and low cost. In recent years, electrodes modified by organic molecules have attracted widespread attention, owing to their good stability, reproducibility, more active sites, homogeneity in electrochemical deposition and strong attachment to electrode surface [26, 27]. Thereinto, organic dyes, such as crystal violet [22], furfural [28], malachite green [29], and thionine [30] have been used for fabricating electrochemical sensors for detecting HQ and CC. As shown in Table 1, the electrodes modified by organic dyes show outstanding electrochemical properties toward the redox of HQ and CC compared with other modified ones. Based on the modification from organic dyes, the larger peak potential difference (ΔE_{pa}) between HQ and CC makes the two isomers be separated more easily, and the lower detection limit of HQ and CC results higher sensitivity, which is appropriate for the quantitative determination of the two isomers. Therefore, it is believed that the electrodes modified with organic dyes can act as potential candidates for simultaneous determination of HQ and CC.

In this paper, an excellent electrochemical activity toward the oxidation of HQ and CC was found on eosin Y film, which was electrodeposited on GCE surface by cyclic voltammetry (CV). The morphology and electrochemical properties of the eosin Y film was characterized by scanning electron microscopy (SEM), CV and electrochemical impedance spectroscopy (EIS). The electrochemical behavior of HQ and CC on eosin Y/GCE was investigated by CV and differential pulse voltammetries (DPV). The results show that the eosin Y exhibits attractive catalytic

performances for simultaneous determination of the two isomers. Further, eosin Y based electrochemical sensor for simultaneous determination of HQ and CC has been constructed. Ultimately, due to its high electroactivity, selectivity and stability, the eosin Y /GCE sensor was applied to the analysis of spiked water sample. To the best of our knowledge, this is the first time that such high sensitivity has been achieved for the simultaneously determination of HQ and CC using eosin Y modified electrode.

2. Experimental

2.1 Apparatus and reagents

Electrochemical experiments such as CV and DPV were performed on a CHI660D electrochemical workstation (Shanghai Chenhua Co., Ltd., China) cabled with a conventional three-electrode cell. A bare or modified GCE was used as the working electrode, and a platinum wire electrode was applied as the counter electrode. A saturated calomel electrode (SCE) worked as the reference electrode. If there is no specific indication, all potentials reported in this paper are quoted with SCE. EIS measurements were performed using PARSTAT2273 (EG&G, USA). An S-2F digital pH meter (Leici instrument factory, Shanghai, China) was used to determine pH value of the buffer solution. The topography of the electrode surface was investigated by a 3-dimensional Hirox KH 8700 Digital Optical Microscope.

All reagents were obtained as analytical grade and used without further purification. Doubly distilled water obtained from a Milli-Q water purification system (18MΩ•cm) was for all experiments. HQ and CC were all analytical grade from Shanghai Chemical Company, China. Eosin Y was purchased from Sigma. Potassium ferricyanide ($K_3[Fe(CN)_6]$) and potassium ferrocyanide ($K_4[Fe(CN)_6]$), sodium phosphate dibasic (Na_2HPO_4), sodium dihydrogen phosphate (NaH_2PO_4), sodium acetate (NaAc) and acetic acid (HAc) were obtained from Beijing Chemical Reagent Factory (Beijing, China). All solutions were freshly prepared before each experiment.

2.2 Preparation of modified electrode

Scheme 1 illustrates the procedure for the construction of eosin Y onto GCE. Firstly,

GCE was polished sequentially with 0.3 and 0.05 μm alumina slurry and then washed ultrasonically in nitric acid (1:1), acetone, ethanol and doubly distilled water for a few minutes, respectively. After rinsing with distilled water, the electrode was endured CV scanning from -0.4 V to 1.6 V in 0.1 M H_2SO_4 at 100 mV/s for 20 cycles [31]. Then the pretreated GCE was obtained. The electrodeposition of eosin Y was carried out under CV sweeping from -1.2 V to 1.5 V at a scan rate of 100 mV/s for 15 cycles. The concentration of eosin Y was 1.0×10^{-3} M in 0.1 M PBS (pH 7.0) and the solution was deoxygenated for 20 min with nitrogen prior to electrodeposition. After that, the eosin Y modified electrode was rinsed sufficiently using double-distilled water to remove the unreacted eosin Y.

2.3 Morphology and electrochemical property of the modified electrodes.

The surface morphology was revealed by a field emission scanning electron microscopy (FE-SEM, Zeiss Ultra 55). The electrochemical property of the electrodes was also evaluated on CHI 660D electrochemical workstation in the aforementioned three-electrode cell. High-purity nitrogen was used for purging oxygen before each experiment. The measurements were carried through at ambient temperature (25±2 ^{o}C). The electrochemical performance of eosin Y/GCE was measured by CV and DPV techniques in acetate solution (pH= 5.0) in the potential range of -0.2 ~ 0.6 V with the scan rate of 100 mV/s. Besides, the electrochemical impedance spectroscopy was performed in 5 mM $Fe(CN)_6^{3-/4-}$ solution containing 0.1 M KCl, and the frequency range was from 10^{-2} to 10^{5} Hz.

3. Results and discussion

3.1 Electrodeposition of eosin Y onto GCE.

Electrodeposition is a facile and efficient approach to immobilize organic film onto solid state electrode surface, since film properties such as thickness, permeation and charge transportation can be adjusted by controlling electrochemical parameters [32]. Fig. 1 shows the successive CV curves during the electrodeposition of eosin Y from a phosphate buffer solution (pH 7.0) containing 1.0×10^{-3} M eosin Y. As can be seen from Fig. 1, two oxidation and reduction peaks are found at the potential of +0.804

V (E_{pa1}), 0.458 V (E_{pa2}), -0.742 V (E_{pc1}) and -1.002 V (E_{pc2}) respectively. During the electrodeposition process, the eosin Y molecules are reduced to free radicals, and combine with the GCE surface rapidly [33]. After fifteen cycles, the peak currents keep constant, so that fifteen cycles are chosen as the representative for the modification process. A uniform film is produced on GCE surface, which indicates that the eosin Y has been deposited on GCE surface by electrodeposition method [34, 35]. According to the detailed research carried through by Yoshida et al [36], the electrochemical reaction of eosin Y, existing as EY^{2-}, will mainly proceed according to Scheme 1 in neutral aqueous solution, and $EY^{3\bullet-}$ free radical is the main product during the electrochemical reduction. Although $EY^{3\bullet-}$ can also react with H^+ to form $EYH^{2\bullet-}$, which will ultimately transform to EYH_2^{2-}, the rate of the subsequent processes is slow, so that the amount of $EYH^{2\bullet-}$ and EYH_2^{2-} is small. It is assumed the deposit is mainly composed by $EY^{3\bullet-}$, which accumulates as the deposit attaching on the surface.

Preferred position for Fig.1

Preferred position for Scheme 1

3.2. Surface morphology characterization

As shown in Fig. 2, SEM technique is employed to reveal the surface morphology of bare GCE and eosin Y/GCE. The surface of bare GCE is very smooth (Fig. 2a). After electrodeposition, the electrode surface is covered by a compact organic dye film (Fig. 2b), which reveals that eosin Y has been deposited on GCE surface. There are many ridges, valleys and craters existing on the surface, which can in return increase the surface area of eosin Y. This unique morphological feature is beneficial because of the large surface area, which will enable the as-modified electrode to act as active platform for the electrocatalysis and electroanalysis of the target molecules.

Meanwhile, the specimen is also investigated by using a three-dimensional optical microscope (Fig. 3). It is shown that a rough eosin Y film is formed on GCE surface

(Fig. 3a), which is corresponding to the SEM characterization. Moreover, as shown in the three dimensional topology (Fig. 3b), the height difference between the highest and lowest sites on the surface can reach *ca*. 6 μm. This rough characteristic can firmly enhance the surface area of the electrode.

Preferred position for Fig.2

Preferred position for Fig.3

3.3 Electrochemcial property of eosin Y/GCE.

EIS is an effective tool to study the electron-transfer phenomena during the electrochemical reaction [37]. In this report, EIS measurements were carried through by using 5.0 mM $Fe[(CN)_6]^{3-/4-}$ as the redox mediator to study the surface property of the pristine and as-modified electrodes. As shown in Fig. 4A, each of the EIS curve includes a well-defined semicircular part at high frequencies and a straight linear part at low frequencies, demonstrating that the electrode process is controlled by electron transfer at high frequencies and by diffusion at low frequencies [38]. The semicircle portion corresponds to the electron-transfer process, and the diameter is equivalent to R_{et}, which is the most direct and sensitive parameter that responds to electrochemical reaction on the electrode and solution interface [26]. The R_{et} from eosin Y/GCE is revealed as 500 Ω, which is much lower than that from bare GCE (1600 Ω). The notable decrease of R_{et} indicates that eosin Y/GCE behaves chemically more active than the primary GCE surface, and the as-formed film can efficiently facilitate the electrochemical reaction. Therefore, the electron transfer kinetic between the target molecules and electrode can be enhanced steadily.

Further, CV curves shown in Fig. 4B prove the enhanced current response on eosin Y/GCE toward $Fe(CN)_6^{3-/4-}$, indicating the increased electrochemical activity. The anodic-to-cathodic peak separation (ΔE_p) for eosin Y/GCE is larger than 59.5 mV, which is attributed to its quasi-reversibility characteristics. The results are in good agreement with the EIS experiments. Moreover, the electrochemically active surface

area can be calculated according to the following equation: $i_p = (2.99\times10^5)n(\alpha n_a)^{1/2}ACD^{1/2}\upsilon^{1/2}$, in which i_p, n, A, C, D and υ represent the peak current, the number of electrons involved in the reaction, the electroactive surface area, reactant concentration, the diffusion coefficient of the reactant species and the scan rate, respectively [39]. Assuming $\alpha = 0.5$ and $n_a = 1$, the redox reaction of $Fe(CN)_6^{3-/4-}$ involves one-electron transfer (n =1), and the diffusion coefficient (D) is 6.30×10^{-6} cm^2 s^{-1} [40]. The values of the electrochemically active surface area for eosin Y/GCE and bare GCE are calculated as 0.144 cm^2 and 0.073 cm^2, respectively. The results reveal that the modified electrode has larger reaction surface area than the unmodified one, which demonstrates that the eosin film can steadily enhance the surface area of the electrode.

Preferred position for Fig.4

3.4 Electrochemical behavior of HQ and CC at modified GCE

The electrochemical behavior of HQ and CC is investigated at eosin Y/GCE and bare GCE in 0.10 M acetate buffer solution (pH 5.0) using CV and DPV techniques. Fig. 5 shows the CV response in the presence of 100 μM HQ and CC at bare and eosin Y modified GCE, respectively. At the bare GCE, the redox peaks of HQ and CC are located at -0.054/0.332 V and 0.066/0.406 V, respectively. In contrast, at the eosin Y/GCE, the redox peaks are measured at 0.082/0.142V and 0.182/0.238 V, and the peak potential differences (ΔE_p) between anodic and cathodic peak (i.e., 60 mV and 56 mV for HQ and CC, respectively) are smaller than those on bare GCE (i.e., 386 mV and 340 mV for HQ and CC, respectively), indicating that the electrochemical reaction reversibility is improved.

CV and DPV response for the mixture of HQ and CC at bare and eosin Y/GCE is shown in Fig. 6. From Fig. 6A(i), bare GCE shows two weak cathodic peaks for HQ and CC, and the oxidation peaks of HQ and CC are overlapped to form a broad anodic peak. For eosin Y/GCE illustrated as Fig. 6A(ii), a pair of well-defined redox peaks can be observed for indicating the existence of both HQ and CC. The anodic and cathodic peak potential differences (denoted as ΔE_{pa} and ΔE_{pc}) between HQ and

CC are up to 111 mV and 103 mV, respectively. Thus, their peaks are well separated and their simultaneous determination can be achieved. Fig. 6B shows DPV response to the mixture of HQ and CC at GCE and eosin Y/GCE. At bare GCE, a small and broad peak is observed. Meanwhile, two well-defined peaks are observed at eosin Y/GCE, and the peak potentials locate at more negative values than those of GCE. Moreover, the peak current increases significantly, and the peak-to-peak separation for HQ and CC reaches about 111 mV. It is well known that the increase in oxidation peak currents, negative shift in oxidation peak potential, and well separation of the oxidation peak at the electrode are prerequisite for simultaneous determination of isomers in mixture solutions [16, 41]. From the above evaluation, it is clear that eosin Y/GCE has higher electrocatalytic activity to the oxidation of HQ (or CC) than that of bare GCE.

Preferred position for Fig.5

Preferred position for Fig.6

3.5 Effect of cycle number during eosin Y deposition on GCE

The thickness of eosin Y film also plays a critical role for the determination of HQ and CC. Film thickness can be effectively controlled by changing the scan cycle number during the electrodeposition process [42]. In this report, the dependency relationship between CV cycle number for eosin Y deposition and HQ (or CC) redox ability is also excavated. Fig. 7 illustrates the variation of electrochemical behavior toward to HQ (or CC) on eosin Y/GCE with different cycle numbers for achieving eosin Y films. In Fig. 7A, when the cycle number for eosin Y deposition adopts 15, E_{pa} and E_{pc} reach the minimum and maximum value, respectively. Meanwhile, oxidation peak currents of HQ (or CC) also arrive at a maximum value in the same case (Fig. 7B). However, when the cycle number increases further, the electrochemical activity of eosin Y film will decrease. Since the as-achieved thick film has higher impedance, it is hard for electrons to penetrate through the layer to

reach the electrode surface [6]. In other words, a very thick or thin film is not beneficial for electrode response. Only optimum thickness originated from reasonable CV cycle number (15 cycles) can enable the lowest ΔE_p and the highest sensitivity.

Preferred position for Fig.7

3.6 Influence of pH to the electroanalytical property

Electrolyte acidity affects electro-oxidation behavior of HQ (or CC), because proton participates in the electrode reaction [31]. In this work, the voltammetric behavior of HQ and CC in different electrolyte solutions, i. e., KH_2PO_4-Na_2HPO_4 (PBS), HAc-NaAc (acetate buffer solution), NaOH-KH_2PO_4, Britton-Robinson buffer solution (B-R) are investigated. The results indicate that well-defined and sensitive peaks are observed in acetate buffer. Thus, the acetate buffer is chosen as the supporting electrolyte in the following study.

CV investigation is carried out to evaluate pH effect to electrochemical behavior of HQ and CC at eosin Y/GCE in the pH range of 3.8~6.0. As shown in Fig. 8A, it is noticeable that with the increasing pH, the peak currents of the two isomers will increase until pH reaches 5.0 and then slightly decrease. These results may be explained by the two reasons as follows: Firstly, it has been reported that the pK_a value of HQ and CC is 9.85 [43] and 9.4 [44], respectively. In high pH range, HQ and CC will gradually de-protonate and turn into anions. Meanwhile, eosin Y on electrode surface is also negatively charged due to trianion radical formation. The electrostatic repulsion between the two isomers and electrode will be enhanced with the increase of pH value, which leads to low adsorption capacity on the electrode surface and low peak current. Secondly, Fig. 8A also illustrates that the oxidation peak (E_{pa}) and reduction peak (E_{pc}) potentials of the two isomers shift to more negative values with the pH increase, which indicates a direct participation of protons in the oxidation process [45, 46]. The solution with high pH value is not advantageous for electrochemical reaction due to the shortage of proton. Therefore,

acetate buffer solution (pH 5.0) was chosen as the optimum pH value for the detection of HQ and CC. Also, Fig. 8B shows the relationship between the anodic peak potential and pH value. The linear equations between E_{pa} and pH are E_{pa} (V) = -0.0603 pH + 0.5288 (R = 0.9951) for HQ and E_{pa} (V) = -0.0611 pH + 0.4237 (R = 0.9884) for CC, respectively. The slope value is 60.3 mV pH^{-1} for HQ and 61.1 mV pH^{-1} for CC, which is close to the theoretical value of -59.0 mV pH^{-1}. It suggests that the ratio of electrons to protons involved in the electrochemical redox process of both HQ and CC is 1. As is known, the electrochemical oxidation of the two isomers is a two-electron process [30]. Thus, the proton numbers involved in the electrochemical oxidations of both HQ and CC should be 2, and the mechanism of the electrooxidation of HQ and CC can be proposed in Scheme 2 [3].

Preferred position for Fig.8

Preferred position for Scheme 2

3.7 Effect of scan rate to the electroanalytical performance

The influence of scan rate on the redox of HQ and CC was further examined on the eosin Y/GCE. CV plots with different scan rates (30.0-240.0 mV s^{-1}) in 50 μM HQ and CC are shown in Fig. 9A. Two pair of well-defined redox peaks appear at different scan rates, and the oxidation peak potentials of HQ and CC are observed to shift positively with increasing the scan rate, which reveals that the electron transfer is quasi-reversible [24]. In addition, both the anodic and cathodic peak currents of HQ and CC enhance with increasing the scan rate. As is shown in Fig. 9B, both the oxidation and reduction peak currents (I_{pa}) are linear to the square root of the scan rate ($\upsilon^{1/2}$). The regression equations are worked out as I_{pa} = -1.605 $\upsilon^{1/2}$ + 1.6845 (μA, mV/s, R = 0.9991) for HQ and I_{pa}= -2.1453 $\upsilon^{1/2}$ + 1.7473 (μA, mV/s, R = 0.9993) for CC, indicating the diffusion-controlled process of HQ and CC at eosin Y/GCE surface [47].

Preferred position for Fig.9

3.8 Interference of coexisting substances

In order to evaluate the selectivity of eosin Y/GCE for determining two phenolic isomers, the possible interference from some inorganic ions and organic compounds is investigated by DPV in acetate buffer solution containing 50 μM HQ and CC. The tolerance limit is defined as the maximum concentration of the foreign substances to cause a *ca.* ±5% relative error in their determination. These results show that 500-fold of Na^+, K^+, NH_4^+, NO_3^-, Zn^{2+}, Ac^-, SO_4^{2-}, Cl^-, 100-fold Ca^{2+}, Mg^{2+}, Al^{3+}, Fe^{3+}, Li^+, Br^-, Cu^{2+}, S^{2-}, glucose, 50-fold concentration of ascorbic acid, uric acid, glycine, L-cysteine, 10-fold L-glutamine, proline, methionine will not show interference to the detection of the two isomers. However, 5-fold phenol, resorcinol interferes the determination due to their co-adsorption at eosin Y/GCE. The above results confirm that the as-modified electrode performs good selectivity.

3.9 Simultaneous determination of HQ and CC.

DPV technique performs higher current sensitivity and better resolution than CV during the electroanalytical application [4]. Thus, by increasing the concentration of one isomer while keeping the concentration of the other isomer constant at 20 μM, the linear range and detection limitation are further studied using DPV technology under the optimum conditions Fig. 10A illustrates that signal of HQ oxidation increases obviously with the increasing of its concentration, while the peak currents of CC at 0.238 V remain constant. The oxidation peak current of HQ is linear to its concentration in the range of 1 μM~130 μM with a regression equation of I_{pa} = -0.1669 c -4.6178 (μA, μM, r=0.9962) (Fig. 10A), and the detection limit is 0.14 μM (S/N = 3). By fixing HQ concentration at 20 μM, the anodic peak current of CC is linear to its concentration in the range of 1 μM~130 μM with a regression equation of I_{pa} = -0.1559 c – 1.6201 (μA, μM, r = 0.9965) (Fig. 10B). The detection limit for CC is 0.12 μM (S/N = 3). The above results reveal that this proposed method can

realize the simultaneous and sensitive determination of HQ and CC without interference to each other. Meanwhile, a comparison of the as-proposed method with other electrochemical approaches is listed in Table 1. It is shown that eosin Y/GCE can lead to a large anodic peak potential difference (ΔE_{pa}) between HQ and CC, which reveals that the two isomers can be separated more easily and the oxidation of dihydroxybenzene isomers in solution mixture occurred independently. By making comparison among the different organic dyes, eosin Y/GCE has slightly larger anodic peak potential difference, i. e., 111 mV, than organic dyes including poly(crystal violet) and poly(thionine), whose value is 108 and 100 mV, respectively. Although eosin Y/GCE has smaller anodic peak potential difference than poly(malachite green) related composite material MWCNT-PMG/GCE (147 mV), the detection limit of the former is more favorable than the later. It indicated that the as-prepared electrode is sensitive and appropriate for the quantitative determination of the two isomers.

Eosin Y/GCE is further demonstrated to be effective for determining both isomers even their concentrations are simultaneously changing. As shown in Fig. 10C (inset), two well-defined anodic peaks are observed, and the peak potential difference is *ca.* 106 mV, which reveals that simultaneous determination of HQ and CC can be achieved at eosin Y/GCE. The anodic peak currents of HQ and CC increase linearly with their own concentration in the range of 1 μM~130 μM. The regression equation is I_{pa} = -0.1408 c – 5.3669 (μA, μM, r=0.9911) for HQ and I_{pa} = -0.1356 c – 3.7255 (μA, μM, r=0.9951) for CC, respectively. Thus, both HQ and CC can be simultaneously determined on eosin Y/GCE with high selectivity and sensitivity.

Preferred position for Fig.10

Preferred position for Table 1

3.10 Reproducibility, stability of the modified electrode

Besides the sensitivity and selectivity, reproducibility and stability are also

considered as two key parameters to assess the applicability of the sensor [1]. Under the optimal conditions, eight eosin Y/GCE are prepared independently, and they are used parallel to determine the oxidation peak current of the mixed solution containing 50 μM HQ and 50 μM CC by DPV technique. The relative standard deviation (RSD) is 3.29% for HQ and 3.47% for CC, indicating the intrinsically good reproducibility. For evaluation the stability of the electrode, after keeping eosin Y/GCE at 4 ^{o}C for three weeks [58], the peak current response is still *ca.* 93.2% of the initial value. It reveals that the as-modified electrode presents an excellent repeatability and durability for determination of HQ and CC.

3.11 Samples analysis

Taking national standard (GB 8978-1996) of China as an example, the permitted emission concentration of phenolic compounds is regulated as 0.5 mg L^{-1} (for dihydroxybenzene, 4.54 $\times 10^{-3}$ M) [44]. According to this value, we have made the spiked solutions having the pollutant concentration much lower than the standard to confirm the practical applicability of the as-prepared electrochemical sensor. Spiked samples containing HQ and CC in local tap water were used to assess the validity of the as-modified electrode. By standard addition method, the DPV responses of the samples were acquired for quantitative determination, and the results are listed in Table 2. Under the optimal experimental conditions, the recoveries are 98.70% ~99.67% and 98.40% ~ 100.2% for HQ and CC, respectively. It indicates that eosin Y/GCE can be used for simultaneous determination of HQ and CC in real water sample.

Preferred position for Table 2

4. Conclusions

In this work, eosin Y film is prepared onto GCE by electrodeposition approach. For the first time, the as-fabricated electrode is proposed to use as an electrochemical sensor for simultaneous determination of HQ and CC. The eosin Y modified glassy carbon electrode is proved to have high electrocatalytic activity and reduce the

oxidation overpotential to HQ and CC. Based on the large peak-to-peak separation between HQ and CC, the simultaneous determination of the two isomers is achieved by DPV technique. This fabricated electrode shows excellent reproducibility, good stability and low detection limit. Based on the obtained results, it is evident that eosin Y/GCE has great potential for HQ and CC determination.

Acknowledgement

The authors are grateful to financial support of the Natural Science Foundation of China (Grant No. 41101223), Natural Science Foundation of Yongchuan (Ycstc,2013nc8001) and Foundation of the Ministry of Education of Chongqing (No. KJ131205).

Reference

[1] K. J. Huang, L. Wang, Y. J. Liu, T. Gan, Y. M. Liu, L. L. Wang, Y. Fan, Electrochim. Acta 107 (2013) 379-387.

[2] W. Liu, L. Wu, X. H. Zhang, J. H. Chen, Anal. Methods, 2013, DOI: 10.1039/c3ay41633j.

[3] L. Z. Zheng, L. Xiong, Y. D. Li, J. P. Xu, X. W. Kang, Z. J. Zou, S. M. Yang, J. Xia, Sensor.Actuat. B-Chem 177 (2013) 344-349.

[4] Z. Q. Hong, L. H. Zhou, J. X. Li, J. Tang, Electrochim. Acta 109 (2013) 671-677.

[5] W. H. Gao, C. L. Quigley, J Chromatogr. A 1218 (2011) 4307-4311.

[6] B. L. Lee, H. Y. Ong, C. Y. Shi, C. N. Ong, J Chromatogr. A, 619 (1993) 259-266.

[7] H. Y. Wang, D. L. Chen, Y. J. Wei, L. Q. Yu, P. Zhang, J. L. Zhao, Spectrochim. Acta A 79 (2011) 2012-2016.

[8] Sirajuddin, M. I. Bhanger, A. Niaz, A. Shah, A. Rauf, Talanta 72 (2007) 546-553.

[9] S.F. Li, X.Z. Li, J. Xu, X.W. Wei, Talanta 75 (2008) 32-37.

[10] S. Dong, L. Chi, Z. Yang, P. He, Q. Wang, Y. Fang, J Sep. Sci 32 (2009) 3232-3238.

[11] A. Judefeind, P. J. V. Rensburg, S. Langelaar, J. D. Plessis, J Chromatogr. B, 852 (2007) 300-307.

[12] H. L. Qi, C. X. Zhang, Electroanal 17 (2005) 832.

[13] G. H. Zhao, Y. T. Tang, M. C. Liu, Y. Z. Lei, X. E. Xiao, Chinese J. Chem 25 (2007) 1445.

[14] S. J. Li, C. Qian, K. Wang, B. Y. Hua, F. B. Wang, Z. H. Sheng, X. H. Xia, Sensor.Actuat. B-Chem 174 (2012) 441-448.

[15] H.J. Du, J. S. Ye, J. Q. Zhang, X. D. Huang, C. Z. Yu, J. Electroanal Chem 650 (2011) 209-213.

[16] Q. H. Guo, J. S. Huang, P. Q. Chen, Y. Liu, H. Q. Hou, T. Y. You, Sensor.Actuat. B-Chem 163 (2012) 179-185.

[17] M. U. A. prathap, B. Satpati, R. Srivastave, Sensor.Actuat. B-Chem 186 (2013) 67-77.

[18] C. H. Bu, X. H. Liu, Y. J. Zhang, L. Li, X. B. Zhou, X. Q. Lu, Colloids Surf B Biointerfaces 88 (2011) 292-296.

[19] X. Wang, M. Wu, H. Li, Q. Wang, P. He, Y. Fang, Sensor.Actuat. B-Chem 192 (2013) 452-458.

[20] G. Y. Xu, B. B. Li, X. L. Luo, Sensor.Actuat. B-Chem 176 (2013) 69-74.

[21] R. M. A. Tehrani, H. Ghadimi, S. A. Ghani, Sensor.Actuat. B-Chem 177 (2013) 612-619.

[22] W. Sun, Y. H. Wang, Y. X. Lu, A. H. Hu, F. Shi, Z. F. Sun, Sensor.Actuat. B-Chem 188 (2013) 564-570.

[23] X. Feng, W. W. Gao, S. H. Zhou, H. Y. Shi, H. Huang, W. B. Song, Anal Chim Acta 805 (2013) 36-44.

[24] X. L. Yuan, D. S. Yuan, F. L. Zeng, W. J. Zou, F. Tzorbatzoglous, P. Tsiakaras, Y. Wang, Appl Catal B 129 (2013) 367-374.

[25] X. Cao, X. Cai, Q. Feng, S. Jia, N. Wang, Anal. Chim. Acta. 752 (2012) 101-105.

[26] D. M. Zhao, X. H. Zhang, L. J. Feng, L. Jia, S. F. Wang, Colloid Surface B 74 (2009) 317-321.

[27] X. Y. Lin, Y. N. Ni, S. Kokot, J Hazard Mater 260 (2013) 508-517.

[28] Y. H. Fu, Y. P. Lin, T. S. Chen, L. S. Wang, J Electroanal Chem 687 (2012) 25-29.

[29] Y. Umasankar, A. P. Periasamy, S. M. Chen, Anal Biochem 411 (2011) 71-79.

[30] A. J. S. Ahammad, M. M. Rahman, G. R. Xu, S. H. Kim, J. J. Lee, Electrochim. Acta 56 (2011) 5266–5271.

[31] P. Y. Shi, X. Q. Miao, H. Yao, S. J. Lin, B. Y. Wei, J. J. Chen, X. H. Lin, Y. H. Tang, Electrochim. Acta 92 (2013) 341-348.

[32] G. Y. Jin, F. Huang, W. Li, S. N. Yu, S. Zhang, J. L. Kong, Talanta 74 (2008) 815-820.

[33] X. Liu, Y. X. Li, S. Q. Peng, G. X. Lu, S. B. Li, Int. J Hydrogen Energ 38 (2013) 11709-11719.

[34] Y. Hong, S. Y. Yuan, L. H. Xin, T. H.Yu, H. Y. Li. Electrochim. Acta 52 (2007) 6165-6171.

[35] P. R. Hu, T. M. Reddy, K. Reddaiah, L. R. Jaidev, G. Narasimha, Enzym Microb Tech 52 (2013) 377-385.

[36] J. B. Zhang, L. N. Sun, T. K. Yoshida, J. Electroanal Chem 662 (2011) 384-395.

[37] X. Y. Sun, S. Hu, L. F. Li, J. Xiang, W. Sun, J Electroanal Chem 651 (2011) 94-99.

[38] Y. P. Dong, L. Z. Pei, X. F. Chu, W. B. Zhang, Q. F. Zhang, Electrochim. Acta 55 (2010) 5135-5141.

[39] C. X. Guo, F. P Hu, C. M. Li, P. K. Shen. Biosensors and Bioelectronics 24 (2008) 819-824.

[40] C. X. Guo, Y. Lei, C. M. Li. Electroanalysis, 2011, 23, 885-893

[41] C. X. Guo, S. R. Ng, S. Y. Khoo, X. T. Zheng, P. Chen, C. M. Li. ACS Nano, 2012, 6, 6944-6951.

[42] Y. F. Peng, Y. P. Ji, D. Y. Zheng, S. S. Hu, Sensor.Actuat. B-Chem 137 (2009) 656-661.

[43] P. D. Astudillo, J. Tiburcio, F. J. Gonzalez, J. Electroanal. Chem. 604 (2007) 57-64.

[44] H. S. Yin, Q. M. Zhang, Y. L. Zhou, Q. Ma, T. Liu, L. S. Zhou, S. Y. Ai, Electrochim Acta 56 (2011) 2748-2753.

[45] X. Y. Lin, Y. N. Ni, S. Kokot, J Hazard Mater 243 (2012) 232-241.

[46] Z. M. Liu, Z. L. Wang, Y. Y. Cao, Y. F. Jing, Y. L. Liu, Sensor.Actuat. B-Chem 157 (2011) 540-546.

[47] W. Sun, Y. Z. Li, M. X. Yang, J. Li, K. Jiao, Sensor.Actuat. B-Chem 133 (2008) 387-392.

[48] X. M. Ma, Z. N. Liu, C. C. Qiu, T. Chen, H. Y. Ma, Microchim Acta 180 (2013) 461-468.

[49] X. Feng, W. W. Gao, S. H. Zhou, H. Y. Shi, H. Huang, W. B. Song, Anal Chim Acta 805 (2013) 36-44.

[50] W. M. Si, W. Lei, Y. H. Zhang, M. Z. Xia, F. Y. Wang, Q. L. Hao, Electrochim Acta 85 (2012) 295-301.

[51] P. F. Bai, G. L. Fan, F. Li, Mater Lett 65 (2011) 2330-2332.

[52] X. Zhang, S. Duan, X.M. Xu, S. Xu, C.L. Zhou, Electrochim Acta 56 (2011) 1981-1987.

[53] D. Zhang, Y. Peng, H. Qi, Q. Gao, C. Zhang, Sensor.Actuat. B-Chem 136 (2009) 113-121.

[54] P. Yang, Q. Zhu, Y. Chen, F. Wang, J Appl Polym Sci 113 (2009) 2881- 2886.

[55] Z. H. Huo, Y. L. Zhou, Q. Liu, X. L. He, Y. Liang, M.T. Xu, Microchim. Acta 173 (2011) 119-125.

[56] L. T. Wang, Y. Zhang, Y. L. Du, D. B. Lu, Y. Z. Zhang, C. M. Wang, J Solid State Electr 16 (2011) 1323-1331.

[57] M. G. Li, F. Ni, Y. L. Wang, S. D. Xu, D. D. Zhang, S. H. Chen, L. Wang, Electroanal 21 (2009) 1521-1526.

[58] C. X. Guo, C. M. Li, Phys. Chem. Chem. Phys., 2010, 12, 12153-12159.

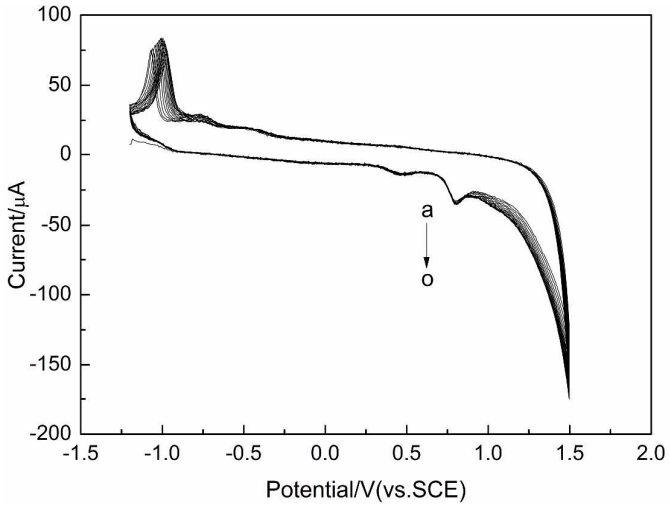

Fig. 1. CV curves during the electrodeposition of eosin Y onto GCE with scan rate 100 mV/s.

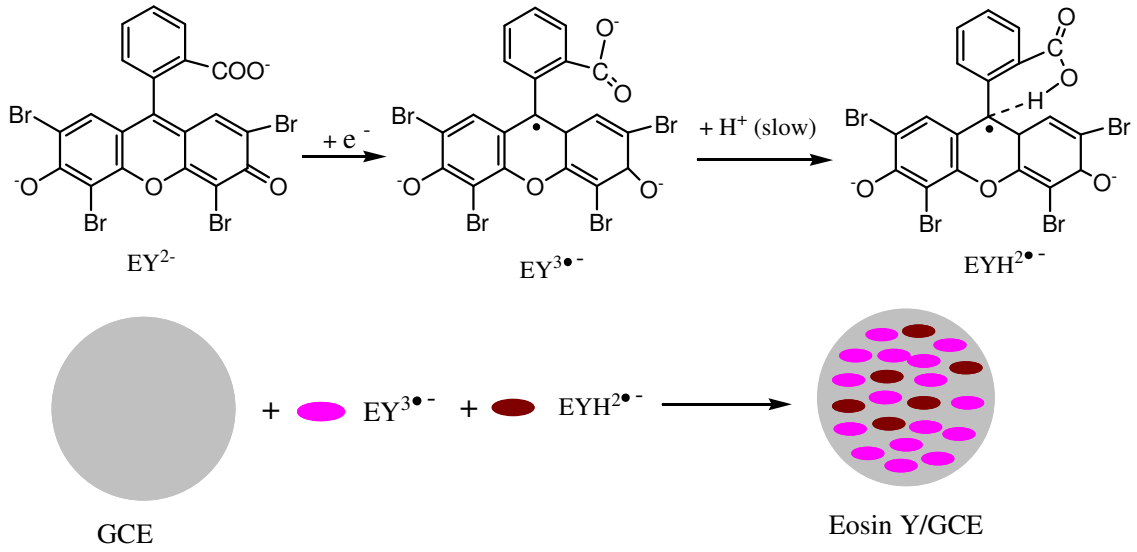

Scheme 1. The modification procedure to get the target electrode.

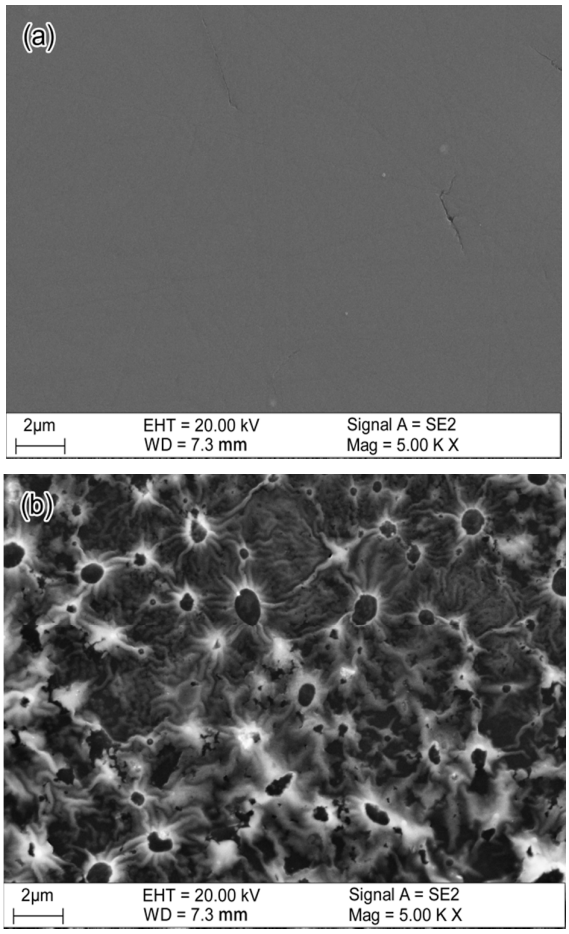

Fig. 2. SEM images of (a) bare GCE (b) eosin Y/GCE.

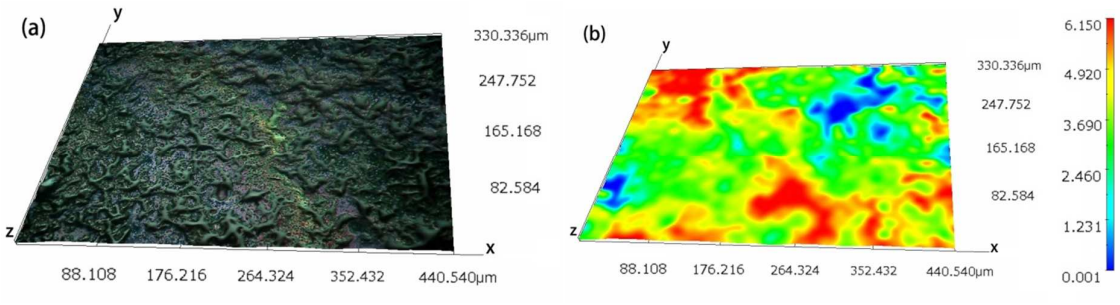

Fig. 3. Optical image of eosin Y film electrodeposited on GCE surface.

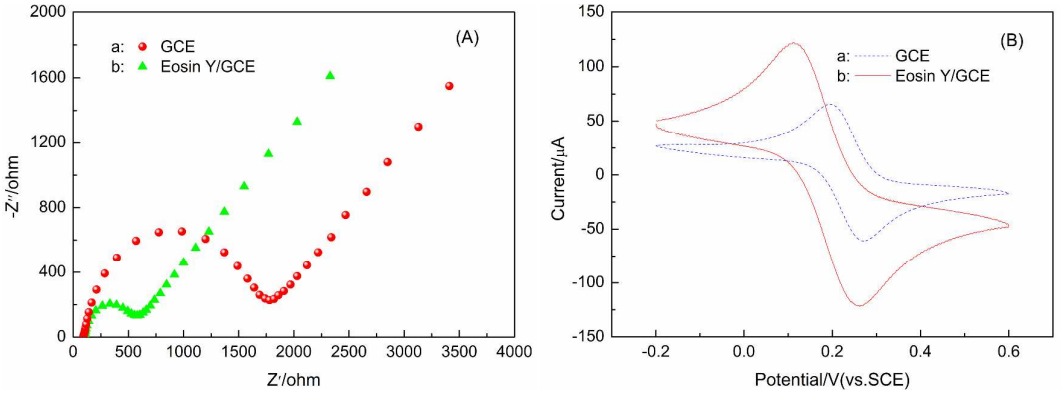

Fig. 4. Nyquist diagram (A) and CV plots (B) of GCE and eosin Y/GCE in 5.0 mM $[Fe(CN)_6]^{3-/4-}$ (1:1) solution containing 0.1 M KCl as supporting electrolyte.

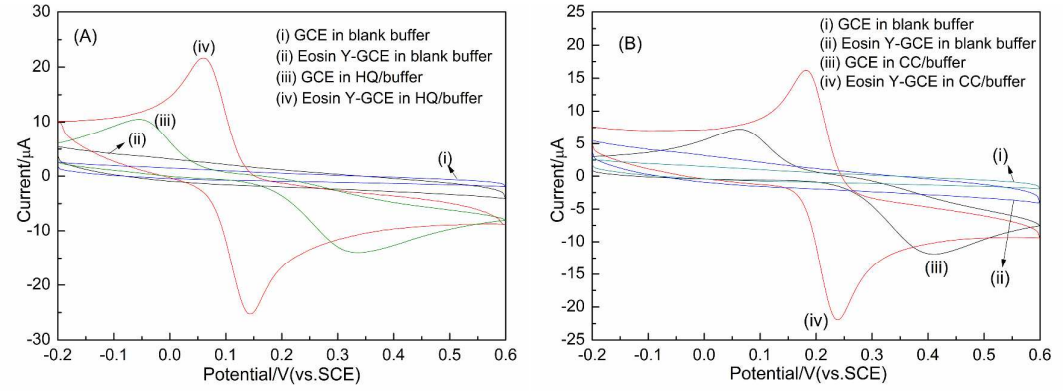

Fig. 5. Electrochemical performance of GCE and eosin Y/GCE in (A) HQ/ HAc-NaAc solution and (B) CC/ HAc-NaAc solution (HAc-NaAc as the buffer). Scan rate during CV scanning is set as 100 mV/s.

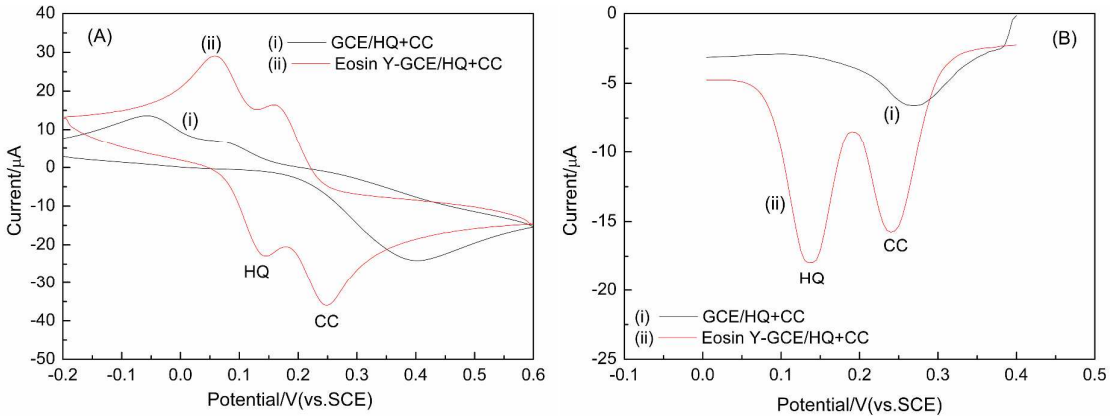

Fig. 6. CV (A) and DPV (B) for the mixture solution of 100 μM HQ and 100 μM CC in acetate buffer solution (pH 5.0) at bare GCE and eosin Y/GCE.

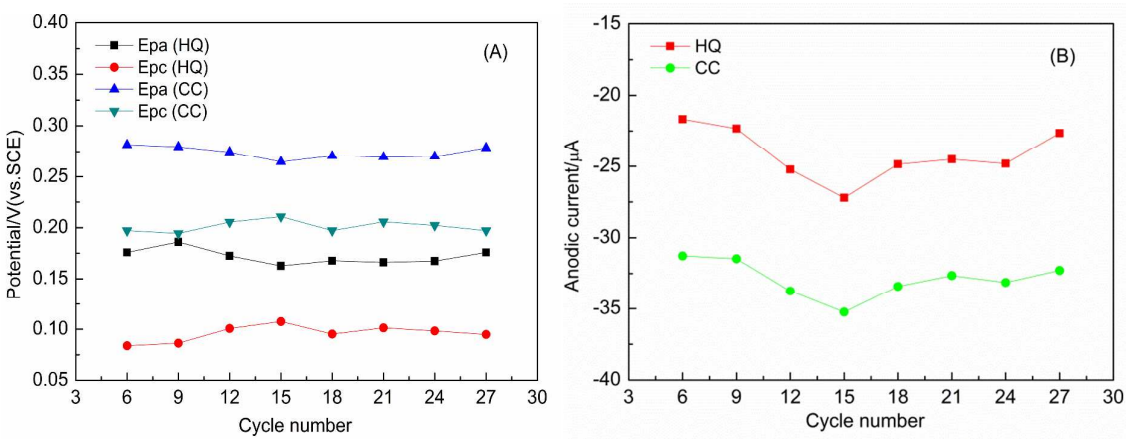

Fig. 7. The relationship of (A) peak potential and (B) oxidation peak current to scan cycle number for eosin Y electrodeposition. The target solution is 100 μM CC/HQ in pH 5.0 HAc-NaAc.

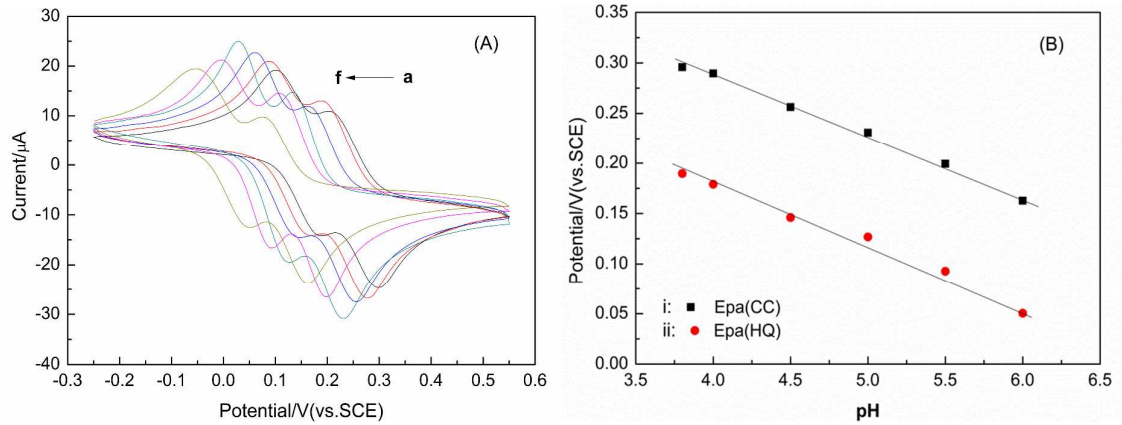

Fig. 8. (A) CV curves of eosin Y/GCE in pH 3.8~6.0 acetate buffer containing a mixture of 100 μM HQ and 100 μM CC (pH value from a to f: 3.8, 4.0. 4.5, 5.0, 5.5, 6.0). (B) E_{pa}-pH relationship of HQ and CC.

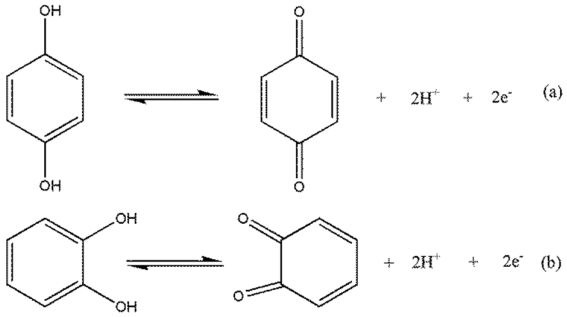

Scheme 2. The electrochemical reaction mechanism of HQ (a) and CC (b).

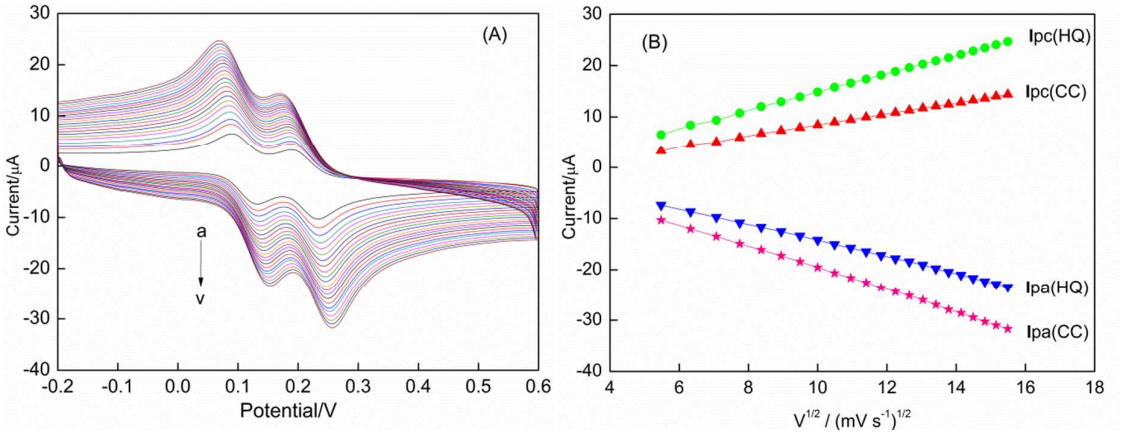

Fig. 9 (A) CVs achieved on eosin Y/GCE with 20 μM HQ and CC in HAc-NaAc (pH 5.0) at different scan rates: a-v: 30, 40, 50, 60, 70, 80, 90, 100, 110, 120, 130, 140, 150, 160, 180, 190, 200, 210, 220, 230, 240 mV/s. (B) The dependence relationship between redox peak current and square root of the scan rate.

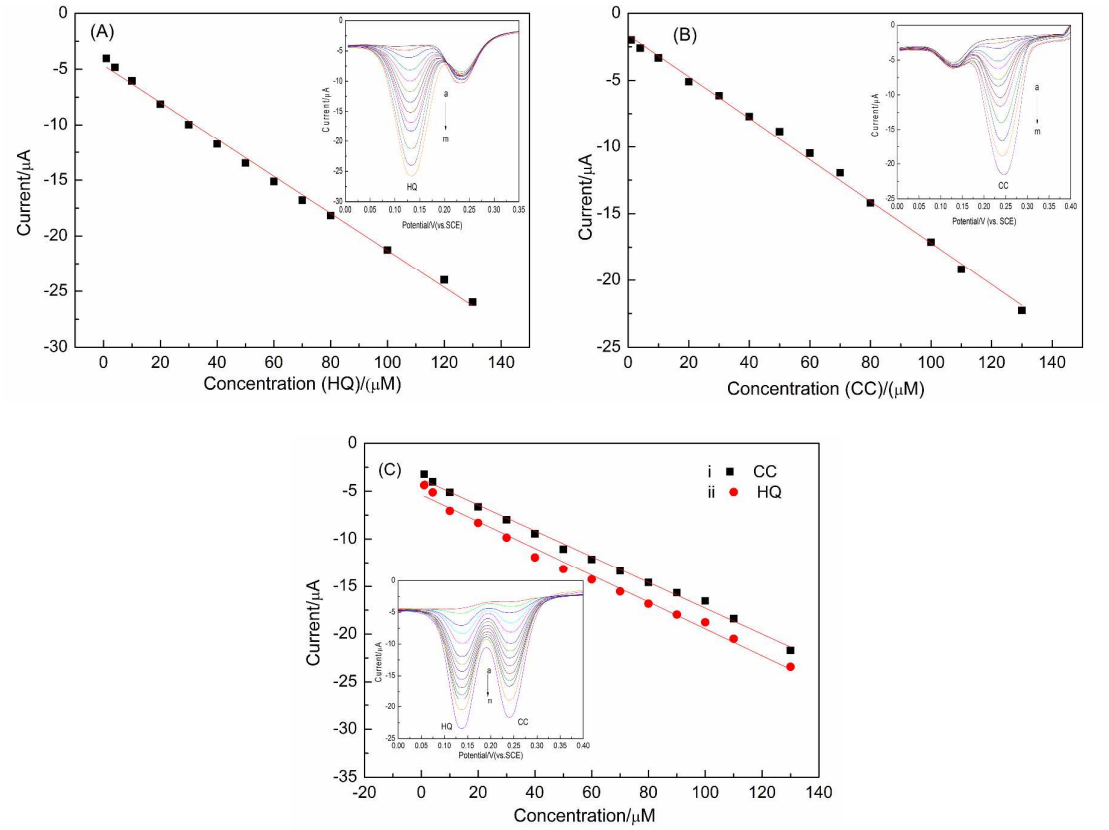

Fig. 10. (A) The calibration plot between HQ concentration and anodic peak current in acetate buffer solution (pH 5.0) containing 20 μM CC and different concentration of HQ. Inset is the DPV curves at eosin Y/GCE. From a to m, concentration of HQ: 1, 5, 10, 20, 30, 40, 50, 60, 70, 80, 100, 120 and 130 μM. (B) The calibration plot between CC concentration and anodic peak current in acetate buffer solution (pH 5.0) containing 20 μM HQ and different concentration of CC. Inset is the DPV curves at eosin Y/GCE. From a to m, concentration of CC: 1, 5, 10, 20, 30, 40, 50, 60, 70, 80, 100, 120 and 130 μM. (C) the calibration curves of HQ and CC. Inset is the DPV of various concentrations of HQ and CC. From a to n, the concentration of HQ and CC is 1, 4, 10, 20, 30, 40, 50, 60, 70, 80, 90, 100, 110 and 130 μM, respectively.

Table 1. Comparison of the electrochemical sensor for HQ and CC detection.

Electrode	Technique	Anodic peak potential difference (mV)	Linear range (μM)		Detection limit (μM)		Reference
			HQ	CC	HQ	CC	
PDA-RGO/GCE	DPV	100	1-250	1-250	0.62	0.74	[3]
ECF-CPE	DPV	108	1-200	1-200	0.2	0.4	[16]
GMC/GCE	DPV	103	1-500	1-400	0.4	0.17	[24]
Grapheme-chitosan/GCE	DPV	100	1-300	1-400	0.75	0.75	[43]
Au-G/GCE	DPV	102	1-100	1-100	0.2	0.15	[47]
PIL-MWCNTs/GCE	DPV	104	1-500	1-400	0.4	0.17	[48]
GO-PEDOT /GCE	DPV	100	2.5-200	2-400	1.6	1.6	[49]
LDH-PCNT/GCE	DPV	100	20-200	10-200	0.54	0.27	[50]
NH_2-SBA15/CPE	DPV	115	0.8-160	1-140	0.3	0.5	[51]
MWNTs/MA	Amperometry	109	1-100	1-100	0.3	0.2	[52]
PPABA/GCE	DPV	104	1.2-600	2-900	0.4	0.5	[53]
GNPs/CNF/Au	DPV	110	9-500	5-350	0.86	0.36	[54]
PDDA-G/GCE	DPV	108	1-500	1-400	0.25	0.2	[55]
LDHf/GCE	DPV	104	12-800	3-1500	9	1.2	[56]
PCV/GCE	DPV	108	0.12-600	0.36-600	0.033	0.097	[22]
MWCNT-PMG/GCE	DPV	147	10-480	30-1190	1.6	5.8	[29]
PTH/GCE	DPV	100	1-120	1-120	0.03	0.025	[30]
Eosin Y/GCE	DPV	111	1-130	1-130	0.14	0.12	This work

[a] PDA-RGO: polydopamine-reduced grapheme oxide; ECF: electrospun carbon nanofiber; PCV: poly(crystal violet); GMC: graphitic mesoporous carbon; PMG: poly(malachite green); PTH: poly(thionine); Au-G: gold-graphene nanocomposite; PIL: polymeric ionic liquid; MWCNTs: multi-walled nanotubes; GO-PEDOT: grapheme oxide doped poly(3,4-ethylenedioxythiophene); LDH-PCNT: Zn-Al layered double hydroxide-poly acrylic acid- functionalized multiwalled carbon nanotubes; NH_2-SBA15/CPE: amino-functionalized SBA-15 mesoporous silicamodified carbon paste electrode; MA: multielectrode array; PPABA: poly-(p-aminobenzoic acid); GNPs/CNF/Au: gold nanoparticle/carbon

nanofibers/Au; PDDA-G: poly(diallyldimethylammonium chloride) functionalized graphene.

LDHf: Zn-Al layered double hydroxide film.

Table 2. Determination results of HQ and CC in spiked water solution samples (n = 6).

samples	Found (μM)		Added (μM)		Total (μM)		RSD (%)		Recovery (%)	
	HQ	CC	HQ	CC	HQ	CC	HQ	CC	HQ	CC
1	9.88	9.91	10.00	10.00	19.81	19.75	2.54	3.32	99.30	98.40
2	9.84	9.97	20.00	20.00	29.58	29.81	3.07	2.61	98.70	99.20
3	9.96	9.89	30.00	30.00	39.86	39.69	2.24	3.86	99.67	99.33
4	9.92	9.85	40.00	40.00	49.57	49.93	3.18	1.95	99.13	100.2

Every primary sample contained HQ (10 μM), CC (10 μM) and some common ions Na^+, K^+, Mg^{2+}, Cu^{2+} and Cl^- in water.